Dalton Transactions

Accepted Manuscript

This is an Accepted Manuscript, which has been through the Royal Society of Chemistry peer review process and has been accepted for publication.

Accepted Manuscripts are published online shortly after acceptance, before technical editing, formatting and proof reading. Using this free service, authors can make their results available to the community, in citable form, before we publish the edited article. We will replace this Accepted Manuscript with the edited and formatted Advance Article as soon as it is available.

You can find more information about Accepted Manuscripts in the author guidelines.

Please note that technical editing may introduce minor changes to the text and/or graphics, which may alter content. The journal's standard Terms & Conditions and the ethical guidelines, outlined in our author and reviewer resource centre, still apply. In no event shall the Royal Society of Chemistry be held responsible for any errors or omissions in this Accepted Manuscript or any consequences arising from the use of any information it contains.

ROYAL SOCIETY OF CHEMISTRY

rsc.li/dalton

Dalton Transactions

PAPER

(Oligo)aromatic species with one or two conjugated Si=Si bonds: near-IR emission of anthracenyl-bridged tetrasiladiene†

Received 00th January 20xx,
Accepted 00th January 20xx

DOI: 10.1039/x0xx00000x

www.rsc.org/

Naim M. Obeid,[a] Lukas Klemmer,[a] Daniel Maus,[b] Michael Zimmer,[a] Jonathan Jeck,[c] Iulia Bejan,[c] Andrew J. P. White,[c] Volker Huch,[a] Gregor Jung,*[,b] and David Scheschkewitz*[,a]

A series of aryl disilenes $Tip_2Si=Si(Tip)Ar$ (**2a-c**) and *para*-arylene bridged tetrasiladienes, $Tip_2Si=Si(Tip)$-LU-$Si(Tip)=SiTip_2$ (**3a-d**) are synthesized by the transfer of the $Tip_2Si=SiTip$ unit to aryl halides and dihalides by nucleophilic disilenides $Tip_2Si=SiTipLi$ (Tip = 2,4,6-$iPr_3C_6H_2$, Ar = aryl substituent, LU = para-arylene linking unit). The scope of the nucleophilic Si=Si transfer reaction is demonstrated to also include substrates of considerable steric bulk such as mesityl or duryl halides Ar-X (Ar = Mes = 2,4,6-$Me_3C_6H_2$; Ar = Dur = 2,3,5,6-Me_4C_6H, X = Br or I). Bridged tetrasiladienes $Tip_2Si=Si(Tip)$-LU-$Si(Tip)=SiTip_2$ with more extended linking units surprisingly exhibit fluorescence at room temperature, albeit weak. DFT calculations suggest that partial charge transfer character of the excited state is a possible explanation.

Introduction

The development of new carbon-based π-systems incorporating heavier main group elements is of considerable interest owing to their potential applications in organic electronics.[1] Due to the inherent high reactivity as well as synthetic challenges, heavier *multiple* bonds have been employed relatively rarely in this context,[2] although after the ground-breaking work of the Protasiewicz and Gates groups[3] multiple bonds to phosphorus or even heavier Group 15 elements enjoy renewed attention recently.[4] Notably, only few reports exist on conjugated systems involving silicon in the conjugation path, although the HOMO-LUMO gap of disilenes is much smaller than that of the corresponding carbon systems.[2d] Disilenes – unlike the carbon-based alkenes – are coloured even in the absence of chromophores and thus show absorptions in the visible region of the electromagnetic spectrum. In addition, the conformational flexibility of the Si=Si bond[2d] can contribute to this trend as the increased admixture of σ- and σ*-orbitals to the π-π* set of orbitals of disilene typically results in a further reduced HOMO-LUMO separation.[5] The availability of functionalized disilenes created new opportunities regarding the exploit of the physical and chemical properties of Si=Si units.[6] In particular, the conjugation of Si=Si bonds with aromatic substituents/spacers was investigated by us[6a,b] and others.[7] The effectiveness of π-conjugation via the organic linking units was shown to be strongly depending on the conformational rigidity of the Si=Si units.[7a] The Si=Si transfer reaction effectuated by lithium disilenide **1** was employed to not only obtain *meta*- and *para*-phenylene bridged tetrasiladienes **I**, but also phenyl-substituted disilenes of type **II** with, in part, residual functionality X (Scheme 1).[6a,b]

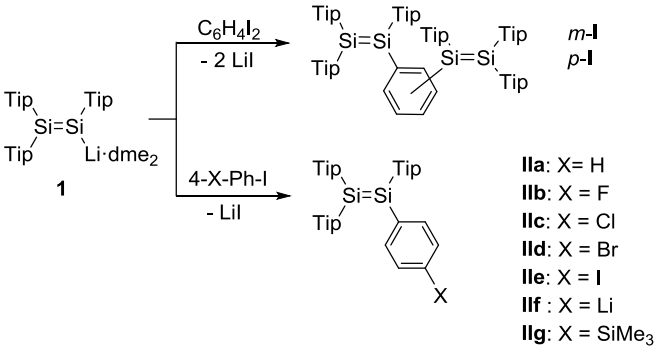

Scheme 1. Synthesis of and phenylene bridged tetrasiladiene m-**I** and p-**I** as well as para-functionalized phenyl-substituted disilenes of Type **II** (Tip = 2,4,6-*i*$Pr_3C_6H_2$).[6a,b]

Just a few months later, Tamao et al. reported on disilene **III** and luminescent *para*-phenylene bridged tetrasiladiene **IV** featuring the very rigid and bulky hindracenyl substituents Eind (Chart 1).[7a] A series of trialkyldisilenes **Va-c** with single polycyclic aromatic substituents (naphthyl, phenanthryl and anthryl) was reported by Iwamoto et al. in 2009 (Chart 1) and shown to exhibit unique metal-to-ligand charge transfer absorptions.[7b] Very recently, Tamao et al. disclosed the synthesis of emissive 1,2-diaryl disilenes with two naphthyl or

[a] *Krupp-Chair of General and Inorganic Chemistry, Saarland University, 66123 Saarbrücken, Germany.*
[b] *Biophysical Chemistry, Saarland University, 66123 Saarbrücken, Germany.*
[c] *Department of Chemistry, Imperial College, Exhibition Road, London SW7 2AZ, United Kingdom..*

† Preliminary results regarding the synthesis of **2a** and **3a** have been published in the PhD theses of I. Bejan (University of Würzburg **2010**) and J. Jeck (Imperial College London **2013**).
Electronic Supplementary Information (ESI) available: Plots of NMR and optical spectra, details on x-ray structures [CCDC-976704 (**2a**), -1529968 (**2b**), -1529974 (**2c**), -1529972 (**2d**), -1529970 (**3a**), -1529971 (**3b**), -1529969 (**3c**), -1529973 (**3d**)] and DFT calculations. See DOI: 10.1039/x0xx00000x

pyrenyl substituents as well as the construction of prototypical OLED devices based on these materials.[8]

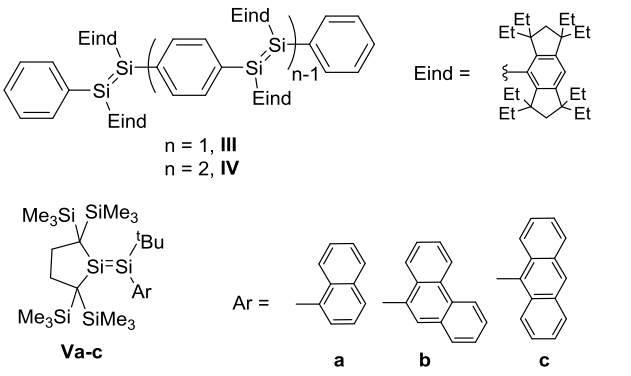

Chart 1. Stable disilenes and tetrasiladienes reported by Tamao[7a] and Iwamoto[7b] groups.

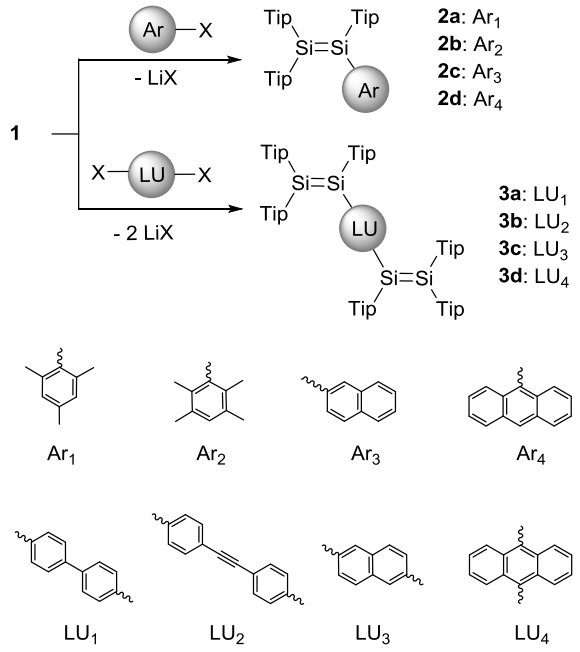

Scheme 2. Synthesis of aryl bridged disilenes **2a-d** and tetrasiladienes **3a-d** with examples of linking units employed in our study (Tip = 2,4,6-iPr$_3$C$_6$H$_2$; X = I or Br).

We herein report the single or double grafting of disilenyl functionalities, Tip$_2$Si=SiTip-, to a broad variety of (poly)aromatic systems as possible organic π-linking units LU (Tip = 2,4,6-iPr$_3$C$_6$H$_2$; Scheme 2) and thus extend the scope of our Si=Si transfer protocol to include sterically rather demanding substrates.

As we will show, the disilenyl group can even be transferred to mesityl (Mes) and duryl substrates (Dur) by reacting the corresponding aryl halides Ar-X with the nucleophilic disilenide **1** if the reaction parameters, namely solvent and temperature, are carefully optimised (Ar = Mes = 2,4,6-Me$_3$C$_6$H$_2$; Ar = Dur = 2,3,5,6-Me$_4$C$_6$H). In contrast, Weidenbruch et al. had reported that the reaction of **1** with MesBr results in its homocoupling to a tetrasilabutadiene.[9] Thus, aryl disilenes **2a-d** and aryl tetrasiladienes **3a-d** were obtained in very good yield and in a broad variety of colours based on the protocol adapted from the preparation of **I** and **II** (Scheme 2).[6a,b] All new compounds are thermally stable in the absence of air and moisture. They were isolated by crystallization and characterized by multinuclear NMR spectroscopy, optical spectroscopy and X-ray diffraction on single crystals. The incorporation of two Si=Si moieties in case of **3b-d** results in fluorescence at room temperature, which is shifted into the near-IR in case of **3d**.

Results and discussion

Synthesis. The slow addition of a pre-cooled benzene solution of one equivalent disilenide **1** to a solution of the different aryl halides (Ar-X) in benzene at about 7°C affords the air-sensitive disilenes **2a-d** as yellow orange (**2a-c**) to purple (**2d**) crystals in 85-88% yield after crystallisation. Following an analogous protocol by treatment of the appropriate aryl dihalides (X-LU-X) with two equivalents of disilenide **1**, the bridged tetrasiladienes **3a-d** were isolated as red (**3a-c**) to blue green (**3d**) crystals in 74% to 94% yield after crystallisation.

Compounds **2a-d** and **3a-d** were investigated by multinuclear NMR analysis and single-crystal X-ray diffraction. Due to its poor solubility in organic solvents, solid state ^{29}Si NMR was additionally performed in case of **3d**. Table 1 summarizes and compares the ^{29}Si NMR data and selected structural parameters determined by X-ray crystallography. Due to unsatisfactory crystal quality of **2d**, only the connectivities could be confirmed, but no bond lengths or angles can be reliably discussed.

Nuclear Magnetic Resonance. In all cases except for **3d**, the quantitative formation of a new Si=Si-containing species was confirmed by the ^{29}Si NMR spectra obtained from the product mixtures. As shown in Table 1, **2a-d** and **3a-c** each show two signals between 52.68 and 71.46 ppm in the typical range for aryl-substituted disilenes.[10] In the ^{1}H NMR spectra of **2b**, the four aromatic protons of the Tip groups at Si2 show individual resonances as doublet signals at δ = 7.09, 7.07, 7.04 and 6.99 ($^{4}J_{H-H}$ = 1.65 Hz) ppm, a clear manifestation of the hindered rotation of the Tip groups at Si2 due to the more pronounced steric bulk at this position. In contrast, the aryl-hydrogen atoms of the Tip group at Si1 of **2b** show just one ^{1}H singlet resonance at δ = 6.97, which confirms the chemical equivalence and thus fast rotation of that group on the NMR time scale. Despite the poor solubility of **3d** and the resulting mediocre signal-to-noise ratio, the ^{29}Si NMR spectrum reveals several weak signals in the range of 52.23 to 62.71 ppm along with two slightly more prominent resonances at δ = 53.94 and 59.71 ppm. Although the absence of signals in the typical area for oxidation or hydrolysis products cannot be confirmed with certainty due to the very bad signal/noise ration of ^{29}Si spectrum in solution, the large number of resonances in the unsaturated region is likely due to the presence of different rotational conformers of **3d**. Unfortunately, it proved impossible to substantiate this assertion by forcing coalescence at elevated temperature due to the insufficient

thermal stability of **3d**. As a consequence, the ^{1}H and ^{13}C NMR spectra of **3d** feature a large number of signals in various intensity ratios, which do not lend themselves to meaningful interpretation (ESI, Figs. S28 and S29). Qualitatively, however, the chemical shift regions in the ^{13}C NMR are in accordance with a CP-MAS ^{13}C NMR spectrum in the solid state (ESI, Fig. S31).

The well-resolved CP-MAS ^{29}Si NMR (ESI, Fig. S32) provides unambiguous prove for the purity of the bulk crystalline material **3d** though. It shows only two signals in at δ = 65.14 and 54.01 ppm (alongside rotational side bands and very minor signals of unknown impurities at δ = −2.25 and −6.30 ppm), which is consistent with the description as tetrasiladiene **3d**. The dilute solution of an aliquot of the batch, proven authentic as **3d** by solid state ^{29}Si NMR, again showed the same set of signals between δ = 52.23 to 62.71 ppm in solution, thus lending the hypothesis of conformational equilibria of **3d** further support.

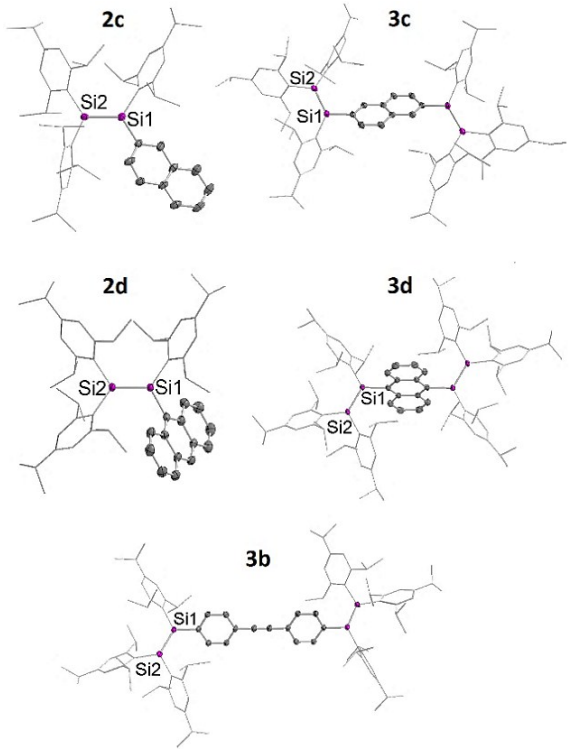

Fig. 1. Molecular structures in the solid state of naphthyl-substituted disilene **2c**, naphthalene-bridged tetrasiladienes **3c**; anthryl-substituted disilene **2d**, anthracene-bridged tetrasiladienes **3d**, acetylene-extended bridged tetrasiladiene **3b** (thermal ellipsoids at 50%, H atoms and disordered *i*Pr groups are omitted for clarity).

X-ray structures. The molecular structures of disilenes **2c,d** and tetrasiladienes **3b-d** are shown in Fig. 1 (see ESI for **2a,b** and **3a**). As the quality of the data set in case of **2d** is insufficient for a discussion of bonding parameters (possibly due to an unresolved twinning issue), it is only taken as proof of constitution. All other compounds have a close to planar geometry about the silicon atoms as the sum of the bond angles at Si1 and Si2 ranges from 357.43 to 359.98°. Variable twisting angles τ are observed for the Si=Si bonds of **2a-c** and **3a-d**, which may simply be taken as a measure of the differing steric congestion (Fig. 1; Table 1; τ = 0.5 to 11.4°). The Si=Si bond distances (2.1453(6) to 2.1622(6) Å) are nevertheless at the short end of the range of literature values for aryl substituted disilenes (2.140 to 2.229 Å).[11] In fact, the Si=Si bonds of all new species are slightly shorter than the corresponding bonds of the less congested phenyl disilene **IIa** and phenyl tetrasiladiene *p*-**I**[6a] (2.1754(11) Å for **IIa** vs. 2.1674(8) Å for *p*-**I**). This somewhat counterintuitive observation can be rationalized by considering the more pronounced *trans*-bending of **IIa** and *p*-**I** compared to that in **2a-c** and **3a-d** (Fig. 2; Table 1; **IIa**: θ_{SiTip} = 23.6°, θ_{SiTip2} = 22.3°; *p*-**I:** θ_{SiTip} = 16.5(2)°, θ_{SiTip2} = 19.3(2)°).[6a] As some of us had previously pointed out, a correlation exists between the sum of *trans*-bent angles and the Si=Si bond length for disilenes with electronically comparable substitution patterns.[6b]

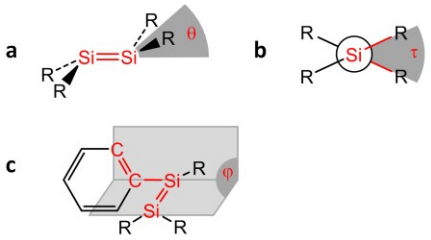

Fig. 2. Illustration of geometrical parameters for Si=Si conjugated systems: (a) *trans*-bent angle θ_{Si} = 90° - (angle between the Si-Si vector and the normal to the plane defined by Si and the pendant substituents), (b) twist angle τ = angle between the normals to the two planes defined by the silicon atoms and the pendant substituents, (c) dihedral distortion from co-planarity given by dihedral angle φ.

Table 1. ^{29}SiNMR data and structural parameters of disilenes **2a-d** and tetrasiladienes **3a-d**.

	2a	**2b**	**2c**	**2d**
δ^{29}Si1 (ppm)	55.76	57.88	71.05	60.08
δ^{29}Si2 (ppm)	55.42	52.95	56.74	52.68
ΣSi1 (°)	359.48	359.3	358.51	-
ΣSi2 (°)	359.41	359.9	359.89	-
Si1-Si2 (Å)	2.1453(6)	2.1516(7)	2.1525(6)	-
θ_{Si1} (°)	6.7	7.5	11.6	-
θ_{Si2} (°)	7.2	1.7	3.2	-
τ (°)	0.5	10.6	10.4	-
φ (°)	50.6	56.3	21.3	-
	3a	**3b**	**3c**	**3d**
δ^{29}Si1 (ppm)	71.04	69.91	71.46	65.14
δ^{29}Si1 (ppm)	65.00	57.52	56.67	54.01
ΣSi1 (°)	359.52	357.43	359.64	359.8
ΣSi2 (°)	359.8	358.86	359.98	359.9
Si1-Si2 (Å)	2.1460(8)	2.1530(8)	2.1622(6)	2.1483(8)
θ_{Si1} (°)	6.7	15.3	5.5	4.7
θ_{Si2} (°)	4.2	9.7	1.3	3.5
τ (°)	11.4	6.4	7.7	1.8
φ (°)	24.8	45.9	38.7	74.6

Notably, **3c** appears to contradict this correlation, which is based on the bonding model developed by Carter, Goddard, Malrieu, and Trinquier (the CGMT model).[12] The naphthalene-bridged tetrasiladiene **3c** shows a unusually long Si=Si bond of 2.1622(6) Å despite the absence of significant *trans*-bending. We suggest this can be taken as an indication of more efficient delocalization of Si=Si π-bonding electron density towards the linking unit. Indeed, the bond distance between silicon and the naphthalene *ipso*-carbon atoms is short compared to that of **2c** (Si-C(ipso) = 1.8700(18) for **2c** vs. 1.8547(19) Å for **3c**). The out-of-plane distortion of the linking unit in **3c** appears to be sufficiently moderate to allow for effective conjugation (φ = 38.7°).

Remarkably, with φ = 74.6° the anthracene-bridged **3d** exhibits the highest torsion angle, approaching orthogonality, which is expected to interrupt the conjugation between Si=Si and the triaromatic linker in **3d** and hence could give rise to an intramolecular charge transfer transition (ICT) from the Si π system to the C π^* system as had been observed by Iwamoto et al. in related species.[7b]

Photophysical properties and Theoretical studies. Disilenes **2a-d** and tetrasiladienes **3a-d** were investigated by UV/Vis spectroscopy, fluorescence spectroscopy and TD-DFT calculations in order to determine the influence of the organic linking unit (LU) on the photophysical properties of the compounds (Table 2).

The disilenes with the monoaromatic substituents **2a** and **2b** (**2a**: Ar = Mes, **2b**: Ar = Dur) show unremarkable longest wavelength absorptions in hexane solution at λ_{max} = 430 nm, which are slightly blue shifted by $\Delta\lambda$ = 9 nm compared to the more *trans*-bent **IIa** (λ_{max} = 439 nm).[6a] In contrast the oligoaromatic substituents of **2c** and **2d** (**2c**: Ar = 2-naphthyl, **2d**: Ar = 9-anthryl) result in a considerable redshift of the longest wavelength absorptions at the expense of progressively reduced extinction coefficients (Table 2). Iwamoto et al. had identified the longest wavelength transition of their 9-antryl substituted disilene **Vc** at λ_{max} = 525 nm as an intramolecular charge transfer (ICT) band with an even smaller extinction coefficient of ε = 480 $M^{-1}cm^{-1}$.[7b] This is undoubtedly a consequence of less efficient conjugation compared to **2d**, an aspect that will be subject to closer inspection by DFT calculations (vide infra).

Table 2. Photophysical data of **2**,**3** and calculated wavelength maxima with HOMO LUMO gap energy of their optimized structure.

	State	λ_{max} (nm)	ε (M^{-1} cm^{-1})	λ_{max}^{exc} (nm)	λ_{max}^{em} (nm)	Φ[%]	$\lambda_{cal.max}$ (nm)	$E_{H\rightarrow L}$ (eV)
2a	Hex	430	21200	-	-	-	-	-
2b	Hex	430	17300	-	-	-	427	2.90
2c	Hex	463	6800	-	-	-	468	2.64
2d	Hex	550	3800	-	-	-	604	2.05
3a	Hex	463	21000	-	-	-	505	2.45
3b	Hex	488	46000	514	570	<0.01	545	2.27
	Solid	-	-	574	619	0.015	-	-
3c	Hex	484	12000	525	574	<0.01	513	2.33
	Solid	-	-	552	587	0.04	-	-
3d	Hex	597	7500	-	-	-	657	1.88
	Solid	-	-	590	816	0.05	-	-

The lowest energy transitions of the bridged tetrasiladienes **3a-c** are as expected more or less red-shifted compared to disilenes with just one Si=Si unit. For **3a**, however, the longest wavelength absorption at λ_{max} = 463 nm is blue-shifted by $\Delta\lambda$ = 45 nm compared to *p*-**I** with a single *para*-phenylene bridge.[6a] The in principle more extended conjugated π-electron system in **3a** is apparently disrupted in solution by the twisting of the two biphenylene aryl rings, which is clearly observable in the solid state structure of **3a**. Indeed, the introduction of an acetylene spacer between the two phenylene moieties as in **3b** results in a red-shift of $\Delta\lambda$ = 25 nm compared to **3a** as well as the by far highest molar extinction coefficient in this series of Si=Si unit containing derivatives (ε = 46000 $M^{-1}cm^{-1}$). The acetylene spacer of **3b** appears to convey an efficient conjugative interaction between the two Si=Si units.

The moderate red shift of $\Delta\lambda$ = 21 nm of the longest wavelength absorption of naphthalene-bridged **3c** (λ_{max} = 484 nm, ε = 12000 $M^{-1}cm^{-1}$) compared to that of naphthyl-substituted **2c** (λ_{max} = 463 nm, ε = 6780 $M^{-1}cm^{-1}$) indicates a slightly less efficient π-conjugation in comparison to that observed between **IIa** and *p*-**I**[6a](Fig. 3). Indeed, the extinction coefficient is only approximately doubled along with the number of Si=Si units and hence of no diagnostic value.

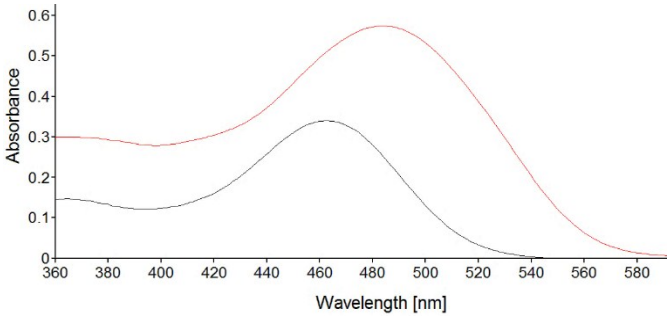

Fig. 3. Normalized UV/Vis spectra of **2c** (Black) and **3c** (Red) in hexane (0.0005 M) at room temperature.

The dominant UV/vis absorption of a hexane solution of **3d** (Fig. 4) at λ_{max} = 422 nm (ε = 36600 $M^{-1}cm^{-1}$) is accompanied by another significantly weaker band at λ_{max} = 597 nm (ε = 7500 $M^{-1}cm^{-1}$), which is red-shifted by $\Delta\lambda$ = 47 nm compared to the corresponding absorption of **2d** at λ_{max} = 550 nm (ε = 3800 $M^{-1}cm^{-1}$). This considerable red-shift together with the extinction coefficients being one order of magnitude larger than that reported for **Vc** suggests that the electronic transition in case of **2d** and **3d** may in fact be best represented by a combination of π-π* and ICT transition despite the inversion symmetry of **3d**.[13] Support for the ICT notion is gathered from the solvent dependency of the absorption bands. In the more polar thf solvent, the longest wavelength bands of **2d** and **3d** are shifted to λ = 568 nm (ε = 4000 $M^{-1}cm^{-1}$) and λ = 621 nm (ε = 8000 $M^{-1}cm^{-1}$), respectively (Fig. 4). Solvatochromic effects are a typical feature of charge transfer transitions,[14] and had also been observed in case of

the mono(disilenyl) substituted **Vc**.[7b] Interestingly, large changes of the static dipole moment upon excitation were previously observed for other non-planar antracene-derivatives.[15] An exhaustive experimental and theoretical treatment of the torsional potential and the symmetry-breaking influence of the solvent, however, is beyond the scope of this study.[16] Both, **2d** and **3d** also exhibit several additional overlapping bands between 300 and 400 nm that can be readily assigned to excitations of the anthracene system itself (e.g. λ_{max} of 9-(pentamethyldisilanyl) anthracene appears at 373 nm[17]).

Given the dihedral distortion of the anthryl group and the Si=Si bonds of **2d** and **3d** a significant mixing of Si=Si and ligand- or bridge-centred orbitals would be unexpected. On the other hand, as had been pointed out before the conformational flexibility of the Si=Si unit in concert with the admixture of σ-electrons could allow for conjugative interactions even in cases when π-orbital overlap is small.[6] Alternatively, the absorption red-shift going from **2d** to **3d** may be an indication of excitonic interaction of the nearby, but not conjugated Si=Si units.

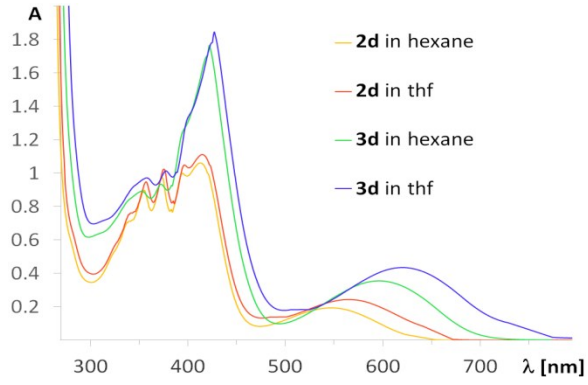

Fig. 4. UV/Vis spectra of **2d** and **3d** in hexane (0.0005 M) and thf (0.0005 M) solution at room temperature.

In order to shed light on these questions, and in particular, to obtain a better understanding of the extended π-conjugation features, possible intramolecular charge transfer and interplay between the two, density functional theory (DFT) calculations were performed at the B3LYP/6-31G(d,p)[18-22] level of theory using the Gaussian09 program package[23] where the Tip groups were simplified to the computationally less demanding Dip groups (Dip = 2,6-*i*Pr$_2$C$_6$H$_3$).

The molecular structure of disilenes **2b-d** and tetrasiladienes **3a-d** determined by X-ray crystallography are reproduced well in the fully optimized structures of **2(b-d)Dip** and **3(a-d)Dip** (see ESI). The calculated Si=Si bond distances of **2(b-d)Dip** and **3(a-d)Dip** are with 2.1675(5) to 2.182(6) Å reasonably close to the experimental values. The anthracene ring is substantially twisted from the Si=Si vector in both **2dDip** and **3dDip** with dihedral angles of φ = 64° and 65°, respectively. In the experimental case in the solid state, **3d** shows a similar geometry with even slightly more twisting φ = 74.6°). For **2d**, the experimental bond lengths or angles in the solid state cannot be reliably discussed due to issues with the quality of the data set. It should be noted, however, that Iwamoto's anthryl disilene **Vc** showed a dihedral distortion of φ = 88° and thus very close to perfect orthogonality of ligand and Si=Si moiety.[7b]

The frontier orbitals for **2(b,d)Dip** and **3(b,d)Dip** are shown in Fig. 5 (for **2cDip** and **3(a,c)Dip** see ESI). The HOMOs predominantly consist of the π(Si-Si) orbital in all cases, with relatively minor participation from the p$_z$ atomic orbitals (AOs) of the organic substituents or bridge. In stark contrast, the LUMO structure differs significantly depending on the nature of the organic moiety.

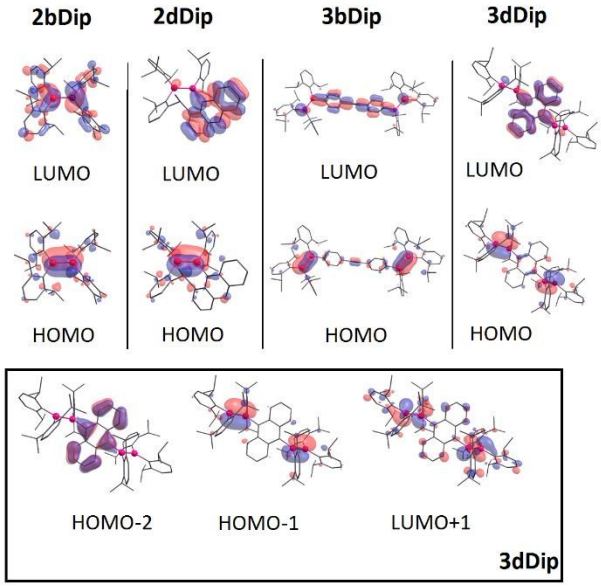

Figure 5. Selected frontier orbitals of disilenes **2(b,d)Dip** and tetrasiladienes **3(c,d)Dip** (isovalue for all orbital plots = 0.03 a.u.).

For the duryl and naphthyl disilenes **2bDip** and **2cDip**, the LUMOs delocalize almost over the entire molecules. In tetrasiladienes **3(a-c)Dip**, the LUMOs equally involve substantial π*(Si–Si)–π*(organic linker) mixing. In contrast, the LUMOs of **2dDip** and **3dDip** are primarily represented by the π*(anthracene) orbital with much less, but nonetheless significant contribution of the π*(Si–Si) orbitals. In fact, an approximate reciprocal relationship between the dihedral twisting of the substituent/linking unit from the plane of the Si=Si units on the one hand and the amount of admixture of Si=Si centred π* orbitals is apparent from visual inspection of the frontier orbitals (Figure 6). This is also in line with Iwamoto's anthryl disilene **Vc** in which the anthryl group was shown to be close to being orthogonal to the Si=Si moiety and consequently no apparent admixture of the Si-Si π* orbitals to the ligand-centred LUMO can be discerned.[7b] Indeed, the two bonding π orbitals HOMO and HOMO−1 of the anthryl-bridged tetrasiladienes **3dDip** are not degenerate (as to be expected for isolated Si=Si bond), but separated by 0.1 eV instead. As shown in Table 2, the HOMO-LUMO gap decreases without exception when increasing the number of repeat Si=Si units

from disilenes **2(c,d)Dip** to tetrasiladiene **3(c,d)Dip**. For instance, in case of naphthalene bridged disilene and tetrasiladiene the resulting overall decrease in the energy gap from 2.64 eV (**2cDip**) to 2.33 eV (**3cDip**) further supports the fact that the π-electron system extends over the two Si=Si units which are in conjugation through the naphthalene linker.

TD-DFT calculations on **2(b-d)Dip** and **3(a-d)Dip** reproduce the absorption spectra of **2b-d** and **3a-d** (see ESI) in a reasonably accurate manner (Table 2). The longest wavelength absorptions thus mainly originate from the HOMO→LUMO transitions.

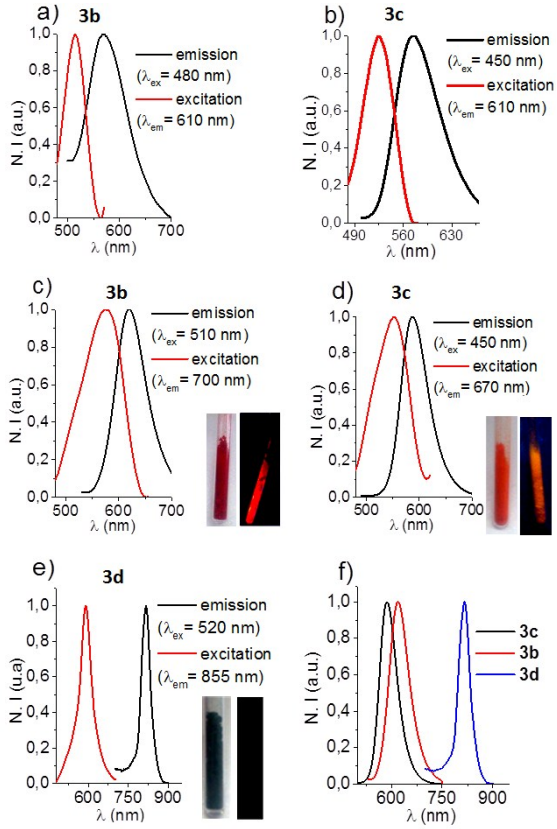

Figure 6. a), b) Excitation and emission spectra of **3b** and **3c** in hexane solution at room temperature; c), d), e) excitation and emission spectra of **3b-d** in solid state at room temperature; f) emission spectra of **3b-d** in solid state at room temperature grouped together for comparison. The inserts show photographic images of the fluorescence caused by a handheld UV-lamp with λ_{max} = 360 nm (dark in case of **3d** due to emission in the near IR).

In contrast to Iwamoto's anthryl disilene,[7b] **3b-d** exhibit fluorescence in solid state (and in hexane solution in case of **3b** and **3c**) at room temperature although the observed quantum yields are very poor, in fact close to the detection limit in some cases (Table 2, Fig. 6). For instance, in hexane at room temperature, **3c** has a maximum wavelength excitation at λ_{max}^{exc} = 525 nm for a detectable emission intensity (λ_{em} = 610 nm), while a maximum emission wavelength (λ_{max}^{em} = 574 nm) occurs at an excitation wavelength of 450 nm. Although the red-shift of the excitation spectra compared to the absorption spectra presumably results from an optical artefact due to the relatively high concentrations used for recording, the emission spectra barely overlap with the absorption spectra and therefore represent the actual transition wavelength from S_1 to S_0. In solid state at room temperature, **3b** shows a red fluorescence with an emission maximum at λ_{max}^{em} = 619 nm, while **3c** exhibits an orange fluorescence with an emission maximum at λ_{max}^{em} = 587 nm close to the solution value. Here, the exact emission wavelength not only depends on the extent of excitonic interaction of neighbouring molecules but also is sensitive to the crystal morphology,[24] and is therefore hardly predictable. The most intriguing feature, however, is certainly the near-IR emission of **3d** with an emission maximum at λ_{max}^{em} = 816 nm. Although near-IR emission at room temperature is a rare phenomenon in main group chemistry in itself,[25] the emission response of **3d** in the solid state is unlikely to be due to impurities as it is clearly related to the absorption maximum at about 600 nm (which was also predicted by TD-DFT calculations). The remarkably large Stokes-shift of $\Delta\lambda$ = 226 nm in **3d** (about 4400 cm^{-1}) compared to **3b** and **3d** and other emissive disilenes[8] may partially result from the closer distance of the two Si=Si units within one molecule providing a larger excitonic splitting due to the r^{-3} dependence.[26] Unusually large Stokes shifts of more than 200 nm in the solid state may also be related to intermolecular coupling.[27] Such shifts can be observed in crystalline entities in dependence of the mutual orientation and strength of the individual, molecular transitions thus modifying the supramolecular emission. The apparent crystalline emission may be further influenced by the morphology of the crystals.[24] As a consequence, the Stokes-shift within a solid is not readily interpretable on a molecular basis and thus beyond the scope of this publication.[28]

Unfortunately, the quality of the emission data was insufficient for the determination of reliable lifetime data for these compounds. The low quantum yields both in solution and solid state of tetrasiladienes **3b-d** are likely due to a rapid non-radiative relaxation of the excited states via the many vibrational modes that can be envisaged for these molecules. On the other hand, the fact that fluorescence can be readily observed, indicates that bulky substituents are appropriate for suppressing these movements and provide a strategy for further enhancement. Indeed, the photoemission of **3b-d** is enhanced in the solid state, presumably due to the restricted motion of substituents.

Conclusions

We have demonstrated that a series of aryl disilenes (**2a-d**) and para-arylene bridged tetrasiladienes (**3a-d)** is accessible from disilenide **1** and the corresponding aryl or arylene (di)halides. Notably, even significant steric demand of the linker does not adversely affect the yields of this reaction. It was found that the electronic communication of bridged disilenyl moieties strongly depends on the overlap of π-orbitals and the conformational freedom of the conjugated scaffold, which can influence the HOMO-LUMO gap significantly. The twisted conformation of the biphenylene in case of **3a** leads to

a lower λ_{max} value compared to tetrasiladiene *p*-**I** although the π-conjugated system is potentially extended. The photophysical data as well as DFT calculations provide strong evidence for the extended π-conjugation through the entire backbone of **2a-b** and **3a-c**. Although intermolecular charge transfer becomes increasingly more relevant when the dihedral distortion of the Si=Si moieties with respect to the organic π-system is increased, there does not seem to exist a clear-cut distinction to the more conventional π-π* transition typical for disilenes in our case. It can be proposed, however, that a more perfect orthogonality (such as observed by the Iwamoto group)[7b] may result in a more intense fluorescence. Indeed, we found that the compounds **3b** and **3c** exhibit fluorescence in solid state and in a hexane solution at room temperature. More importantly, with the anthryl-substituted **3d** the first example of a room temperature near infrared-emissive Si=Si species has been obtained.

Experimental

General considerations. All manipulations were carried out under a protective atmosphere of argon applying standard Schlenk or glovebox techniques. Solvents were dried and degassed by reflux over sodium/benzophenone under argon. C_6D_6 was dried over sodium or potassium, and then distilled under argon. $Tip_2Si=Si(Tip)Li\cdot 2dme$ **1** (Tip= 2,4,6-triisopropylphenyl) was prepared according to published procedures. All other chemicals were obtained commercially and used as supplied.

^1H and ^{13}C NMR spectra were referenced to residual signals of the solvent. ^{29}Si spectra were referenced to external $SiMe_4$. UV/Vis spectra were acquired using a Perkin-Elmer Lambda 35 spectrometer using quartz cells with a path length of 0.1 cm. The fluorescence spectra were recorded using a Jasco Spectrofluorometer FP-6500. The fluorescence quantum yields were measured by a Hamamatsu Quantaurus-QY Absolute PL Quantum Yield Spectrometer C11347. Melting points were determined under argon in sealed NMR tubes and are uncorrected. Elemental analyses were performed on a Leco CHN-900 analyzer.

General procedure for the preparation of disilenes 2a-d and tetrasiladienes 3a-d. A 7°C cold benzene solution of the required stoichiometric amount of disilenide is added dropwise to a solution of the appropriate aryl halide or aryl dihalides in benzene using a dropping funnel pre-cooled with ice water in the cooling mantle. During the addition period of 2h care is to be taken that the temperature of both dropping funnel and receiving flask is kept at 7°C. The reaction mixture is brought to room temperature and stirred for additional 22 hours. All volatiles are removed in vacuum and the residue is digested in hexane. Insoluble material (LiX) is separated from the solution by filtration. Crystallization from a minimum amount of the indicated solvent affords the corresponding product.

1-Mesityl-1,2,2-tris(2,4,6-triisopropylphenyl)disilene (2a). Quantities: MesBr (0.14 g, 0.72 mmol) in 20 ml of benzene, lithium disilenide **1** (0.62 g, 0.72 mmol) in 20 ml of benzene. Isolation: Yellow orange pure solid product after removal of solvent, 0.52 g (93%, mp. 160°C, no dec.) and single crystals of **2a** are grown from hexane. Characterization: **^{1}H NMR** (300 MHz, [D_6]benzene, TMS) δ 7.08 (s, 3H, Tip-*H*); 7.02 ,7.00, 6.98 (each s, each 1H, Tip-*H*); 6.67, 6.65 (s, 2H, Mes-*H*); 4.64 (hept., ^{3}J(H,H) = 6.7 Hz 1H, ^{i}Pr-C*H*), 4.53 (hept., ^{3}J(H,H) = 6.6 Hz, 2H, ^{i}Pr-C*H*); 3.81 (hept., ^{3}J(H,H) = 6.7 Hz, 3H, ^{i}Pr-C*H*); 2.72 (hept., ^{3}J(H,H) = 6.7 Hz, 3H, ^{i}Pr-C*H*); 2.66, 2.53, 2.02 (s, each 3H, Me-*H*); 1.46, 1.45, 1.44, 1.42, 1.40, 1.18, 1.17. 1.16, 1.15, 1.13, 0.72, 0.70, 0.66, 0.63, 0.58 (each d, ^{3}J(H,H) = 6.7 Hz, altogether 54H, iPr-CH_3) ppm. **^{13}C NMR** (75.46 MHz, [D_6]benzene, TMS) δ 155.83, 155.44, 155.40, 155.11, 155.00, 154.43 (Tip-C_o); 150.75, 150.69, 150.49 (Tip-C_p);144.56, 143.85 (Mes-C_p); 138.57 (Mes-C_o); 137.79 (Mes-C_i); 134.79, 134.43, 132.16 (Tip-C_i); 128.62, 128.17 (Mes-C_m); 122.48, 122.40, 122.25, 121.41, 121.25, 121.21 (Tip-C_m); 39.00, 38.53, 38.20, 37.04, 36.76, 36.34, 34.55, 34.52, 34.46 (^{i}Pr-*C*H); 25.85, 25.76 (Me-C_o); 25.18, 25.14, 25.07, 24.76, 24.73, 24.60, 24.47, 24.34, 24.11, 24.05, 24.02, 23.99, 23.91 (^{i}Pr-*C*H_3); 21.13 (Me-C_p) ppm. **^{29}Si NMR** (59.62 MHz, [D_6]benzene, TMS) δ 55.95 (*Si*PhTip); 55.58 (*Si*Tip_2) ppm. UV-Vis(hexane) λ_{max} (ε) 430 nm (21200 $M^{-1}cm^{-1}$); **Exact mass (EI)**: found, 784.5800; calcd for C_{54} H_{80} Si_2, 784.5799.

1-(2,3,5,6-Tetramethylphenyl)-1,2,2-tris(2,4,6-triisopropylphenyl)disilene (2b). Quantities: 1-Iodo-2,3,5,6-tetramethylbenzene (0.85 g, 3.27 mmol) in 30 ml of benzene, disilenide (2.79 g, 3.27 mmol) in 35 ml of benzene. Isolation: Yellow crystals at room temperature from hexane, 2.30 g (88%, mp. 145°C, dec.). Characterization: **^{1}H NMR** (300 MHz, [D_6]benzene, TMS) δ 7.09, 7.07, 7.04, 6.99 (each d, each 1H, ^{4}J = 1.65 Hz; Tip-*H*); 6.97 (s, 1H, Tip-*H*); 6.77 (s, 1H, $C_6Me_4H_1$); 4.60, 4.49, 3.80 (each hept., each 2H, iPr-C*H*); 2.76, 2.70, 2.68 (hept., each 1H, iPr-C*H*); 2.73, 2.54, 1.95, 1.90 (each s, each 3H, $C_6Me_4H_1$); 1.43 (d, 3H, iPr-CH_3); 1.37 (d, 3H, iPr-CH_3); 1.30 (s, 3H, iPr-CH_3); 1.27-1.24 (m, 14H, iPr-CH_3); 1.22 (d, 3H, iPr-CH_3); 1.20 (d, 3H, iPr-CH_3); 1.18 (s, 2H, iPr-CH_3); 1.08-0.99 (m, 14H, iPr-CH_3); 0.77, 0.63, 0.52 (each d, 9H, iPr-CH_3) ppm. **^{13}C NMR** (75.46 MHz, [D_6]benzene, TMS) δ 155.68, 155.52, 155.12, 154,68, 150.76, 150.06 (Tip-*Co/p*), 139.96, 139.28, 134.12, 133.97, 133.46, 132.75 (Ar-C_i); 133.05 (Ar-*C*H); 127.80, 127.54 ($C_6Me_4H_1$-C_q); 122.53, 122.39, 122.33, 121.43, 121.28, 121.15 (Tip-*C*H); 38.92, 38.57, 38.25, 36.97, 36.62, 36.47 (iPr-*C*H); 34.57, 34.51, 34.41 ($C_6Me_4H_1$-*C*H_3); 25.19, 24.77, 24.39, 24.11, 23.99, 23.44, 22.80, 20.73, 20.32 (iPr-*C*H_3) ppm. **^{29}Si NMR** (59.62 MHz, [D_6]benzene, TMS) δ 57.88 (*Si*Tip); 52.95 (*Si*Tip_2) ppm. UV-Vis (hexane) λ_{1max} (ε_1) 335 nm (15000 $M^{-1}cm^{-1}$); λ_{2max} (ε_2) 430 nm (17300 $M^{-1}cm^{-1}$); Combustion Analysis: Calcd. for $C_{55}H_{82}Si_2$: C, 82.63; H, 10.34. Found: C, 82.52; H, 10.26.

1-(Naphthalen-2-yl)-1,2,2-tris-(2,4,6-triisopropylphenyl)disilene (2c). Quantities: 2-bromonaphtalene (0.37 g, 1.79 mmol) in 25 mL of benzene, disilenide (1.53 g, 1.79 mmol) in 25 ml of benzene. Isolation: red orange crystals at room temperature from hexane, 1.21 g (85%, mp. 120°C, dec.). Characterization: **^{1}H NMR** (300 MHz, [D_6]benzene, TMS) δ 7.90 (s, 1H, Si-$C_{10}H_7$); 7.43 (t, 2H, Si-$C_{10}H_7$); 7.30 (d, 2H, Si-$C_{10}H_7$), 7.15, 7.09, 7.06 (each s, each 2H, Tip-*H*); 7.07 (d, 1H, Si-$C_{10}H_7$); 7.04 (br., 1H, Si-$C_{10}H_7$); 4.34,

4.27, 4.06 (each hept., each 2H, iPr-C*H*); 2.70, 2.75, 2.70 (each hept., each 1H, iPr-C*H*); 1.23, 1.20, 1.17, 1.14, 1.26, 1.09, 1.07 (each d, altogether 54H, iPr-CH_3) ppm. **^{13}C NMR** (75.46 MHz, [D_6]benzene, TMS) δ 156.32, 156.07, 155.68, 155.06, 151.68, 151.15, 150.63 (Tip-*Co/p*); 136.32 ($C_{10}H_7$-*C*H); 136.29 ($C_{10}H_7$-C_i); 133.79, 133.47, 133.13, 133.01, 130.16 (Tip-C_i); 132.47, 129.69, 129.29 ($C_{10}H_7$-*C*H); 127.87, 127.55 ($C_{10}H_7$-$C_{q.}$); 126.99, 126.14, 124.83 ($C_{10}H_7$-*C*H); 121.97, 121.62 (Tip-*C*H); 38.27, 38.14, 37.34, 34.76, 34.60, 34.51, 34.41 (iPr-*C*H); 25.59, 24.55, 24.14, 23.97, 23.82 (iPr-*C*H_3) ppm. **^{29}Si NMR** (99.36 MHz, [D_6]benzene, TMS) δ 71.05 (*Si*Tip); 56.74 (*Si*Tip_2) ppm. UV-Vis (hexane) λ_{max} (ε) 463 nm (6800 $M^{-1}cm^{-1}$); Combustion Analysis: Calcd. for $C_{55}H_{76}Si_2$: C, 83.26; H, 9.66. Found: C, 83.51; H, 9.77.

1-(Anthracen-9-yl)-1,2,2-tris(2,4,6-triisopropylphenyl)disilene (2d). Quantities: 9-bromoanthracene (0.38 g, 1.49 mmol) in 20 mL of benzene, of disilenide (1.273 g, 1.49 mmol) in 25 ml of benzene. Isolation: Purple crystals at −26°C from pentane, 2.30 g (87%, mp. 168°C, dec.). Characterization: **^{1}H NMR** (300 MHz, [D_6]benzene, TMS) δ 9.75 (d, 1H, Si-$C_{14}H_9$); 9.09 (d, 1H, Si-$C_{14}H_9$); 8.18 (s, 1H, Si-$C_{14}H_9$); 7.73, 7.66 (each d, each 1H, Si-$C_{14}H_9$); 7.27-7.18, 7.12-7.11, 7.10-7.03 (each m, each 2H, Tip-*H*); 7.01, 6.93, 6.84, 6.68 (each s, each 1H, Si-$C_{14}H_9$); 5.03, 4.67, 4.31 (each hept., each 1H, iPr-C*H*); 4.03 (hept., 2H, iPr-C*H*); 3.81, 2.75, 2.65, 2.51 (each hept., each 1H, iPr-C*H*); 1.68, 1.53, 1.33, 1.30, 1.76, 1.10, 0.98, 0.84, 0.61, −0.06, −0.39 (each d, altogether 54H, iPr-CH_3) ppm. **^{13}C NMR** (75.46 MHz, [D_6]benzene, TMS) δ 156.02, 155.54, 155.29, 155.20, 155.17, 154.37, 151.01, 150.98 (Tip-$C_{o/p}$); 137.69, 137.14, 136.46 ($C_{14}H_9$-C_i); 133.32, 133.20, 132.31, 131.51 (Tip-C_i); 131.46, 130.02, 129.16, 129.01, 128.40, 128.37 ($C_{14}H_9$-*CH*); 127.87, 127.55 ($C_{14}H_9$-$C_{q.}$); 125.61, 125.40 ($C_{14}H_9$-*C*H); 122.64, 122.47, 122.28, 121.55, 121.47, 121.28, 121.05 (Tip-*C*H); 39.18, 38.65, 38.43, 37.80, 36.64, 36.45, 34.63, 34.53, 34.25 (iPr-*C*H); 25.65, 25.23, 24.84, 24.76, 24.65, 24.15, 24.04, 23.99, 23.84, 23.75, 23.62, 23.32 (iPr-*CH*$_3$); 34.49, 22.54, 14.11 (pentane) ppm. **^{29}Si NMR** (59.62 MHz, [D_6]benzene, TMS) δ 60.08 (*Si*Tip); 52.68 (*Si*Tip_2) ppm. UV-Vis (hexane) λ_{max} (ε) 373 nm (19500 $M^{-1}cm^{-1}$), 412 nm (21500 $M^{-1}cm^{-1}$), 550 nm (3800 $M^{-1}cm^{-1}$); Combustion Analysis: Calcd. for $C_{59}H_{78}Si_2$: C, 84.02; H, 9.32. Found: C, 84.17; H, 9.46.

4,4´-Bis{1,2,2-[tris(2,4,6-triisopropylphenyl)]}disilenylbiphenyl (3a). Quantities: 4,4´-diiodobiphenyl (0.237 g, 0.585 mmol) in 20 ml of benzene, disilenide (1g, 1.17 mmol) in 20 ml of benzene. Isolation: Red crystals at room temperature from hexane, 0.75 g (88%, mp. 178°C, dec.). Characterization: **^{1}H NMR** (300 MHz, [D_6]benzene, TMS) δ 7.35 (d, 4H, -(C_6H_4)$_2$-); 7.13, 7.10, 7.03 (each s, each 4H, Tip-*H*); 6.99 (d, 4H, -(C_6H_4)$_2$-); 4.29, 4.20, 4.0, 2.76 (each hept., each 4H, iPr-C*H*); 2.69 (hept., 2H, iPr-C*H*); 1.24, 1.22, 1.18, 1.14, 1.12, 1.04 (each d, altogether 108H, iPr-CH_3) ppm. **^{13}C NMR** (75.46 MHz, [D_6]benzene, TMS) δ 156.19, 155.59, 155.09, 154.97, 151.55, 151.15, 150.54, 148.92 (Tip-$C_{o/p}$); 140.75, 137.41 ((C_6H_4)$_2$-C_i); 136.37 ((C_6H_4)$_2$-*C*H); 133.34, 133.19, 130.24 (Tip-C_i); 127.86, 127.54 ((C_6H_4)$_2$-$C_{q.}$); 126.12 ((C_6H_4)$_2$-*C*H); 122.22, 121.92, 121.53 (Tip-*C*H); 38.25, 38.06, 37.43, 34.75, 34.58, 34.40 (iPr-*C*H); 25.95, 24.51, 24.28, 24.15, 24.29, 23.99, 23.80 (iPr-*C*H_3) ppm. **^{29}Si NMR** (59.62 MHz, [D_6]benzene, TMS) δ 71.04 (*Si*Tip); 56.00 (*Si*Tip_2) ppm. UV-Vis (hexane) λ_{1max} (ε_1) 277 nm (35000 $M^{-1}cm^{-1}$); λ_{2max} (ε_2) 463 nm (21000 $M^{-1}cm^{-1}$); Combustion Analysis: Calcd. for $C_{102}H_{146}Si_4$: C, 82.44; H, 9.83. Found: C, 82.60; H, 9.97.

1,2-Bis(4-(1,2,2-tris(2,4,6-triisopropylphenyl)disilenyl)phenyl)ethyne (3b). Quantities: bis(4-bromophenyl)acetylene (0.296 g, 0.88 mmol) in 20 ml of benzene, disilenide (1.60 g, 1.87 mmol) in 23 ml of benzene. Isolation: Red crystals at room temperature from benzene, 1.25 g (94%, mp. 184°C, dec.). Characterization: **^{1}H NMR** (300 MHz, [D_6]benzene, TMS) δ 7.25 (d, 4H, -C_6H_4-); 7.11; 7.08; 7.032 (each s, each 4H, Tip-*H*); 7.02 (d, 4H, -C_6H_4-); 4.24, 4.17, 3.98, 2.76 (each hept., each 4H, iPr-C*H*); 2.69 (hept., 2H, iPr-C*H*); 1.20, 1.19, 1.16, 1.15, 1.13, 1.10 1.06; 1.04 (each d, altogether 108H, iPr-CH_3) ppm. **^{13}C NMR** (75.46 MHz, [D_6]benzene, TMS) δ 156.20, 155.54, 155.05, 151.69, 151.38, 150.72 (Tip-*Co*/p); 139.55 (C_6H_4-C_i); 135.75 (C_6H_4-*C*H); 132.92, 132.69, 129.88, 123.50 (Tip-C_i); 130.88 (C_6H_4-*C*H); 127.87, 127.55 (C_6H_4-$C_{q.}$); 121.97, 121.60 (Tip-*C*H); 91.43 (Carbon-Carbon.triple bond); 38.26, 38.21, 37.34, 34.74, 34.59, 34.39 (iPr-*C*H); 25.51, 24.51, 24.11, 23.99, 23.93, 23.87 (iPr-*C*H_3) ppm. **^{29}Si NMR** (59.62 MHz, [D_6]benzene, TMS) δ 69.91 (*Si*Tip); 57.52 (*Si*Tip_2) ppm. UV-Vis (hexane) λ_{1max} (ε_1) 309 nm (47700 $M^{-1}cm^{-1}$); λ_{2max} (ε_2) 488 nm (46000 $M^{-1}cm^{-1}$); Combustion Analysis: Calcd. for $C_{104}H_{146}Si_4$: C, 82.72; H, 9.67. Found: C, 77.55; H, 9.12. Combustion analysis did not yield satisfactory results presumably due to the oxygen sensitivity of **3b**.

2,6-Bis{1,2,2-[tris(2,4,6-triisopropylphenyl)]}disilenyl naphthalene (3c). Quantities: 2,6-dibromonaphthalene (0.22 g, 0.73 mmol) in 25 ml of benzene, disilenide (1.32 g, 1.54 mmol) in 22 ml of benzene. Isolation: Red crystals at room temperature from benzene, 0.79 g (74%, mp. 150°C, dec.). Characterization: **^{1}H NMR** (300 MHz, [D_6]benzene, TMS) δ 7.67 (s, 2H, -$C_{10}H_6$-); 7.27(d, 2H, -$C_{10}H_6$-); 7.12, 7.06, 7.04 (each s, each 4H, Tip-*H*); 6.75 (d, 2H, -$C_{10}H_6$-); 4.28, 4.24, 4.05, 2.77 (each hept., each 4H, iPr-C*H*); 2.68 (hept., 2H, iPr-C*H*); 1.24, 1.22, 1.18, 1.14 (br.), 1.12, 1.06 (each d, altogether 108H, iPr-CH_3) ppm. **^{13}C NMR** (75.46 MHz, [D_6]benzene, TMS) δ 156.25, 155.594, 155.06, 151.67, 151.02, 150.61 (Tip-$C_{o/p}$); 136.65 ($C_{10}H_6$-C_i); 136.06 ($C_{10}H_6$-*CH*); 133.18, 133.15, 130.22 (Tip-C_i); 132.43, 128.42 ($C_{10}H_6$-*C*H); 127.87, 127.55 ($C_{10}H_6$-$C_{q.}$); 127.12 ($C_{10}H_6$-CH); 122.3, 121.91, 121.52 (Tip-*C*H); 38.32, 38.06, 37.43, 34.75, 34.58, 34.41 (iPr-*C*H); 25.61, 24.51, 24.28, 24.15, 24.29, 23.99, 23.82 (iPr-*C*H_3) ppm. **^{29}Si NMR** (59.62 MHz, [D_6]benzene, TMS) δ 71.46 (*Si*Tip); 56.67 (*Si*Tip_2) ppm. UV-Vis (hexane) λ_{max} (ε) 484 nm (12200 $M^{-1}cm^{-1}$); Combustion Analysis: Calcd. for $C_{100}H_{144}Si_4$: C, 82.35; H, 9.95. Found: C, 75.49; H, 9.07. Combustion analysis did not yield satisfactory results presumably due to the oxygen sensitivity of **3c**.

9,10-Bis{1,2,2-[tris(2,4,6-triisopropylphenyl)]}disilenylanthracene (3d). Quantities: 9,10-dibromoanthracene (0.98 g, 2.92 mmol) in 80 ml of benzene, disilenide (5g, 5.86 mmol) in 80 ml of benzene. Isolation: dark blue-green microcrystals at −10°C from THF, 3.89 g (88%, mp. 189°C, dec.) and single crystals of **3d** are grown from benzene. Characterization: **^{29}Si NMR** (59.62 MHz,

[D_6]benzene, TMS) δ 63.08; 62.65; 60.19; 59.71; 54.63; 53.94; 53.49 ppm. **CP-MAS ^{29}Si NMR** (79.49 MHz) δ 65.14; 54.01; (very minor signals at −2.25; −6.30 ppm of unknown impurities). UV-Vis (hexane) λ_{1max} (ε_1) 422 nm (36600 $M^{-1}cm^{-1}$); λ_{2max} (ε_2) 597 nm (7500 $M^{-1}cm^{-1}$); Combustion Analysis: Calcd. for $C_{104}H_{146}Si_4$: C, 82.80; H, 9.75. Found: C, 79.27; H, 8.04. Combustion analysis did not yield satisfactory results presumably due to the oxygen sensitivity of **3d.**

Theoretical studies. Optimized structures as well as orbitals from natural bond orbital (NBO)[26,27] analysis were visualized with the ChemCraft[28] program. Data from TD-DFT calculations was processed and visualized with the GaussSum[29] and OriginPro 2016G[30] programmes.

Acknowledgements

The authors thank Prof. Dr. Todd Marder and Dr. Lei Ji (University of Würzburg) for many fruitful discussions. Financial support for this study was provided by the Deutsche Forschungsgemeinschaft (DFG SCHE906/5-1), the Alfried Krupp von Bohlen und Halbach-Foundation, and COST Action CM1302 (Smart Inorganic Polymers).

Notes and references

1 a) S. Parke, M. Boone and E. Rivard, *Chem. Commun.,* 2016, **52**, 9485-9505; b) M.P. Duffy, W. Delaunay, P.-A. Bouit and M. Hissler, *Chem. Soc. Rev.,* 2016, **45**, 5296-5310; c) A. C. Grimsdale and K. Müllen, *Macromol. Rapid Commun.,* 2007, **28**, 1676-1702; d) M. Hissler, P. W. Dyer and R. Reau, *Top. Curr. Chem*., 2005, **250**, 127-163 e) M. Hissler, P. W. Dyer and R. Reau, *Coord. Chem. Rev.,* 2003, **244**, 1-44.

2 a) C. Präsang and D. Scheschkewitz, *Chem. Soc. Rev.,* 2016**, 45***,* 900-921; b) A. M. Priegert, B. W. Rawe, S. C. Serin and D. P. Gates, *Chem. Soc. Rev.*, 2016, **45**, 922-953; c) M. C. Simpson and D. Protasiewicz, *Pure Appl. Chem.,* 2013, **85**, 801-815; d) D. Scheschkewitz, *Chem. Lett*. 2011**, 40,** 2-11; e) T. Matsuo, M. Kobayashi and K. Tamao, *Dalton Trans.,* 2010, **39**, 9203-9208; f) D. Scheschkewitz, *Chem. Eur. J.,* 2009, **15**, 2476-2485.

3 a) V. A. Wright and D. P. Gates, *Angew. Chem.*, 2002, **114**, 2495-2498; *Angew. Chem. Int. Ed.,* 2002, **41**, 2389-2392; b) R. C Smith and J. D. Protasiewicz, *J. Am. Chem. Soc.,* 2004, **126**, 2268-2269; c) V. A. Wright, B. O. Patrick, C. Schneider and D. P. Gates, *J. Am. Chem. Soc.,* 2006, **128**, 8836-8844.

4 a) D. M. Salazar, E. Mijangos, S. Pullen, M. Gao and A. Orthaber, *Chem. Commun.,* 2017, **53**, 1120-1123; b) A. Arkhypchuk, A. Orthaber and S. Ott, *Eur. J. Inorg. Chem*. 2014, 1760-1766*;* c) A. Arkhypchuk, M-P. Santoni and S. Ott, *Angew. Chem. Int Ed.,* 2012, **51**, 7776-7780, d) B. Li, T. Matsuo, D. Hashizume, H. Fueno, K. Tanaka and K. Tamao, *J. Am. Chem. Soc.,* 2009, **131**, 13222-12223.

5 M. Kira, *Organometallics,* 2011, **30**, 4459-4465.

6 a) I. Bejan and D. Scheschkewitz, *Angew. Chem.,* 2007*,* **119***,* 5885-5888*; Angew. Chem. Int Ed.,* 2007, **46**, 5783-5786; b) J. Jeck, I. Bejan, A. J. P. White, F. Breher and D. Scheschkewitz, *J. Am. Chem. Soc.* 2010, **132**, 17306-17315; c) M. Majumdar, V. Huch, I. Bejan, A. Meltzer and D. Scheschkewitz, *Angew. Chem. Int Ed.,* 2013, **52**, 3516-3520.

7 a) A. Fukazawa, Y. Li, S. Yamaguchi, H. Tsuji and K. Tamao, *J. Am. Chem. Soc.* 2007*,* **129***,* 14164-14165; b) T. Iwamoto, M. Kobayashi, K. Uchiyama, S. Sasaki, S. Nagendran, H. Isobe and M. Kira, *J. Am. Chem. Soc.,* 2009, **131**, 3156-3157, c) L. Li, T. Matsuo, D. Hashizume, H. Fueno, K. Tanaka and K. Tamao, *J. Am. Chem. Soc.,* 2015, **137**, 15026-15035.

8 a) M. Kobayashi, T. Matsuo, D. Hashizume, H. Fueno, K. Tanaka and K. Tamao, *J. Am. Chem. Soc.* 2010, **132**, 15162-15163; b) K. Tamao, M. Kobayashi, T. Matsuo and H. Tsuji, *Chem. Commun.,* 2012, **48**, 1030–1032. c) M. Kobayashi, N. Hayakawa, T. Matsuo, B. Li, T. Fukunaga, H. Fueno, K. Tanaka and K. Tamao, *J. Am. Chem. Soc.* 2016, **138**, 758-761.

9 M. Weidenbruch, S. Willms, W. Saak and G. Henkel, *Angew. Chem.,* 1997, **109**, 2612-2613; *Angew. Chem., Int. Ed. Engl.,* 1997, **36**, 2503-2504.

10 D. Auer, C. Strohmann; A. V. Arbuznikov and M. Kaupp, Organometallics, 2003, **22**, 2442-2449.

11 I. J. Bruno, J. C. Cole, M. Kessler, J. Luo, W. D. S. Motherwell, L. H. Purkis, B. R. Smith, R. Taylor, R. I. Cooper, S. E. Harris and A.G. Orpen, *J. Chem. Inf. Comput. Sci*., 2004, **44**, 2133-2144.

12 (a) E. A. Carter and W. A. Goddard III, *J. Phys. Chem.,* 1986, **90**, 998-1001; (b) G. Trinquier and J. P. Malrieu, *J. Am. Chem. Soc.,* 1987, **109**, 5303-5315; (c) J. P. Malrieu and G. Trinquier, *J. Am. Chem. Soc.,* 1990, **94**, 6184-6196.

13 R. Wortmann, K. Elich, S. Lebus and W. Liptay, *J. Chem. Phys.,* 1991, **95**, 6371-6381.

14 P. Chen and T. J. Meyer, *Chem. Rev.,* 1998, **98**, 1439−1477.

15 R. Wortmann, S. Lebus, K. Elich, S. Assar, N. Detzer and W. Liptay, *Chemical Physics Letters.,* 1992, **198**,220-228.

16 F. C. Grozema, M. Swart, R. W. J. Zijlistra, J. J. Piet, D. A. Siebbeles and P. Van Duijnen., *J. Am. Chem. Soc.,* 2005, **127**, 11019-11028.

17 Y. Sato, Y. Ueki, M. Ishikawa and M. Kumada, *J. Chem. Soc., Faraday Trans.,* 1984, **80**, 341.

18 A. D. Becke, *J. Chem. Phys.* 1993, **98**, 5648-52.

19 R. Ditchfield, W. J. Hehre and J. A. Pople, *J. Chem. Phys.,* 1971, **54**, 724-728.

20 W. J. Hehre, R. Ditchfield and J. A. Pople, *J. Chem. Phys.,* 1972, **56**, 2257-2261.

21 M. M. Francl, W. J. Pietro, W. J. Hehre, J. S. Binkley, M. S. Gordon, D. J. DeFrees and J. A. Pople, *J. Chem. Phys.,* 1982, **77**, 3654-3665.

22 V. A. Rassolov, *J. Comput. Chem.,* 2001, **22**, 976-984.

23 M. J. Frisch, G. W. Trucks, H. B. Schlegel, G. E. Scuseria, M. A. Robb, J. R. Cheeseman, G. Scalmani, V. Barone, B. Mennucci, G. A. Petersson, et al., *Gaussian 09 Revision B*.

24 C. Spies, A.-M. Huynh, V. Huch and G. Jung, *J. Phys. Chem. C*, 2013, **117**, 18163-18169.

25 C. Stoumpos, D. Malliakas and G. Kanatzidis*, Inorg. Chem.,* 2013, **52**, 9010-9038.

26 M. Kasha, H. R. Rawls and M. A. El-Bayoumi, *Eighth European Congress on Molecular Spectroscopy*, Copenhagen 1965, 371-392.

27 R. M. Hochstrasser, Rev. Mod. Phys., 1962, **34**, 531-549.

28 It was nonetheless attempted to optimize (and thus relax) the vertically excited state of the model system **3dDip**. A preliminary assessment of this computationally demanding calculations after one week (and thus the first few cycles) suggested an instability of the wave function and the attempt was therefore abandoned.

29 J. P. Foster and F. J. Weinhold, *J. Am. Chem. Soc.,* 1980, **102**, 7211-7218.

30 A. E. Reed, L. A. Curtiss and F. Weinhold, *Chem. Rev.,* 1988, **88**, 899-926.

31 http://www.chemcraftprog.com

32 N. M. O'Boyle, A. L. Tenderholt and K. M. Langner, *J. Comp. Chem.* 2008, **29**, 839-845.

33 http://www. OriginLab.com.